Origins of Individual Swimming Behavior in Bacteria

Matthew D. Levin,* Carl J. Morton-Firth,* Walid N. Abouhamad,# Robert B. Bourret,# and Dennis Bray*
*Department of Zoology, University of Cambridge, Cambridge CB2 3EJ, United Kingdom, and #Department of Microbiology and Immunology, University of North Carolina, Chapel Hill, North Carolina 27599-7290 USA

ABSTRACT Cells in a cloned population of coliform bacteria exhibit a wide range of swimming behaviors—a form of non-genetic individuality. We used computer models to examine the proposition that these variations are due to differences in the number of chemotaxis signaling molecules from one cell to the next. Simulations were run in which the concentrations of seven gene products in the chemotaxis pathway were changed either deterministically or stochastically, with the changes derived from independent normal distributions. Computer models with two adaptation mechanisms were compared with experimental results from observations on individuals drawn from genetically identical populations. The range of swimming behavior predicted for cells with a standard deviation of protein copy number per cell of 10% of the mean was found to match closely the experimental range of the wild-type population. We also make predictions for the swimming behaviors of mutant strains lacking the adaptational mechanism that can be tested experimentally.

INTRODUCTION

If you watch them closely, tethered by their flagellae to the surface of an antibody-coated slide, you can tell them from each other by the way they twirl, as accurately as though they had different names.

Lewis Thomas, Medusa and the Snail

The term "non-genetic individuality" has been applied to organisms from a genetically identical population that display differences in phenotype from individual to individual. This phenomenon has been observed repeatedly in both prokaryotic and eukaryotic organisms (McAdams and Arkin, 1997). The individuality in the swimming behavior of *Escherichia coli* (Spudich and Koshland, 1976) is of particular interest because the underlying cell signaling pathway is uniquely well characterized in terms of the concentrations of the components and the rate constants of the reactions in which they participate. This has spurred the development of a number of computer models of chemotaxis that illuminate particular aspects of the pathway (Bray et al., 1993; Bray and Bourret, 1995; Hauri and Ross, 1995; Barkai and Leibler, 1997; Spiro et al., 1997).

Motility in a coliform bacterium is generated by up to six motors attached to long filamentous flagella. When the motors rotate in a counterclockwise direction, the flagella form a bundle and the cell swims smoothly (runs) with a high degree of directionality. On the other hand, when the motors rotate in a clockwise direction, the flagellar bundle flies apart and the cell tumbles, randomly reorienting the direction of the subsequent run (reviewed in Eisenbach, 1990). The behavior of a flagellar motor is commonly quantified in terms of its *bias*, defined as the fraction of time that the motor rotates in a counterclockwise direction. Movement of a cell up a concentration gradient of attractant increases the bias of the motors and, hence, the persistence of movement in this favorable direction (Block et al., 1983), with the result that the cell performs a biased random walk toward the source of attractant (Berg and Brown, 1972).

In 1976, Spudich and Koshland described the pronounced differences that exist in the swimming behavior of individual cells in a cloned population of bacteria (Spudich and Koshland, 1976). They gave the cells, which were either free-swimming or tethered to the surface of microscope coverslips by antibodies to individual flagella, a brief chemotactic stimulus of attractant and measured their adaptational response—the time taken to return to the original pattern of runs and tumbles. The cells showed major and persistent differences in their individual adaptation times, as well as related differences in their resting-state pattern of runs and tumbles. These differences were independent of nutritional state and position of the cell in its division cycle.

In their original paper, Spudich and Koshland proposed that the variations could be generated by stochastic fluctuations in small numbers of molecules controlling the direction of flagellar rotation. The identity of these molecules was not known at the time, but now, two decades later, we have detailed information not only on the proteins themselves but also on their average numbers in the cell and their functions in controlling the rotation of flagella. It is, therefore, possible to use detailed computer models of the signal pathway to survey, in a systematic fashion, how changes in the number of signaling molecules, either singly or coordinately with other proteins, influence flagellar rotation. We can also ask whether some proteins have a greater effect than others and whether certain mutants, especially those affecting the adaptational response, may be expected to show more or less individual variation.

Received for publication 7 July 1997 and in final form 29 September 1997.

Address reprint requests to Dr. Matthew Levin, Department of Zoology, University of Cambridge, Downing Street, Cambridge CB2 3EJ, UK. Tel.: 44(0)1223336623; Fax: 44(0)1223336676; E-mail: mdl22@cus.cam.ac.uk.

Walid N. Abouhamad's present address is Laboratory of Pharmacology and Chemistry, National Institute of Environmental Health Sciences, Research Triangle Park, NC 27709.

0006-3495/98/01/175/07 $2.00

METHODS

Signal pathway

The chemotactic response pathway consists of a set of transmembrane receptor proteins (e.g., Tar) and the products of four chemotaxis genes, CheW, CheA, CheY, and CheZ. The latter four convey information on the binding of attractants or repellents at the receptors to the flagellar motor, and thereby modify its direction of rotation (reviewed in Parkinson, 1993; Eisenbach, 1996; Stock and Surette, 1996). The receptors are bound in a complex to the autophosphorylating protein kinase CheA via the linking protein CheW. Phosphoryl groups are transferred from phosphorylated CheA, CheAp, to CheY, and phosphorylated CheY, CheYp, then diffuses to the switch complex of the flagellar motor, causing a reversal in the direction of rotation from counterclockwise (the default direction) to clockwise. CheZ terminates the response by stimulating the dephosphorylation of CheYp. Two other gene products are involved in adaptation of the chemotactic response: the methyltransferase CheR methylates up to six specific sites on each receptor, and the methylesterase CheB performs the reverse demethylation reaction. The phosphorylation of CheB to CheBp, again by phosphotransfer from CheAp, causes a large increase in its esterase activity (Fig. 1).

Theory

A detailed computer model of the signal response pathway in bacterial chemotaxis has been described previously (Bray and Bourret, 1995). This model includes the phosphorylation reactions in which CheYp is formed, together with the network of binding steps through which the active receptor complex (TTWWAA) is assembled from the starting material of Tar dimers (TT), CheW monomers (W), and CheA dimers (AA). For the purposes of the present study, we have expanded the model to implement the adaptation reactions mediated by CheR and CheB in both a "robust" and a "fine-tuned" manner. Robust systems intrinsically maintain certain properties, for example exact adaptation, when the system parameters—concentration and kinetic data—vary over a wide range. In fine-tuned systems, however, the system parameters are adjusted, usually through an optimization procedure, to obtain the desired property, which is likely to be lost when even small changes in the system parameters are made.

In the implementation of the "fine-tuned" algorithm, the rates of the adaptation reactions depend solely on the current concentrations of modified or unmodified receptor according to bimolecular mass-action laws. This mechanism is similar to one originally proposed by Segel et al. (1986) and later used in a more detailed fashion by Hauri and Ross (1995) and Spiro et al. (1997). In the implementation of the second "robust" algorithm (a copy of the robust version of the program is available from the website http://www.zoo.cam.ac.uk/zoostaff/levin/index.htm), the receptor is assumed to exist in either an active or an inactive conformation depending on its ligand occupancy and state of methylation (Asakura and Honda, 1984). Methylation by CheR in this case occurs at a constant rate, whereas demethylation by CheB takes place only when the receptor is in its active state. It has been shown that under these conditions the system will always return to its original level of activity regardless of the nature or magnitude of the stimulus or the rate constants or concentrations of the reactants (Barkai and Leibler, 1997).

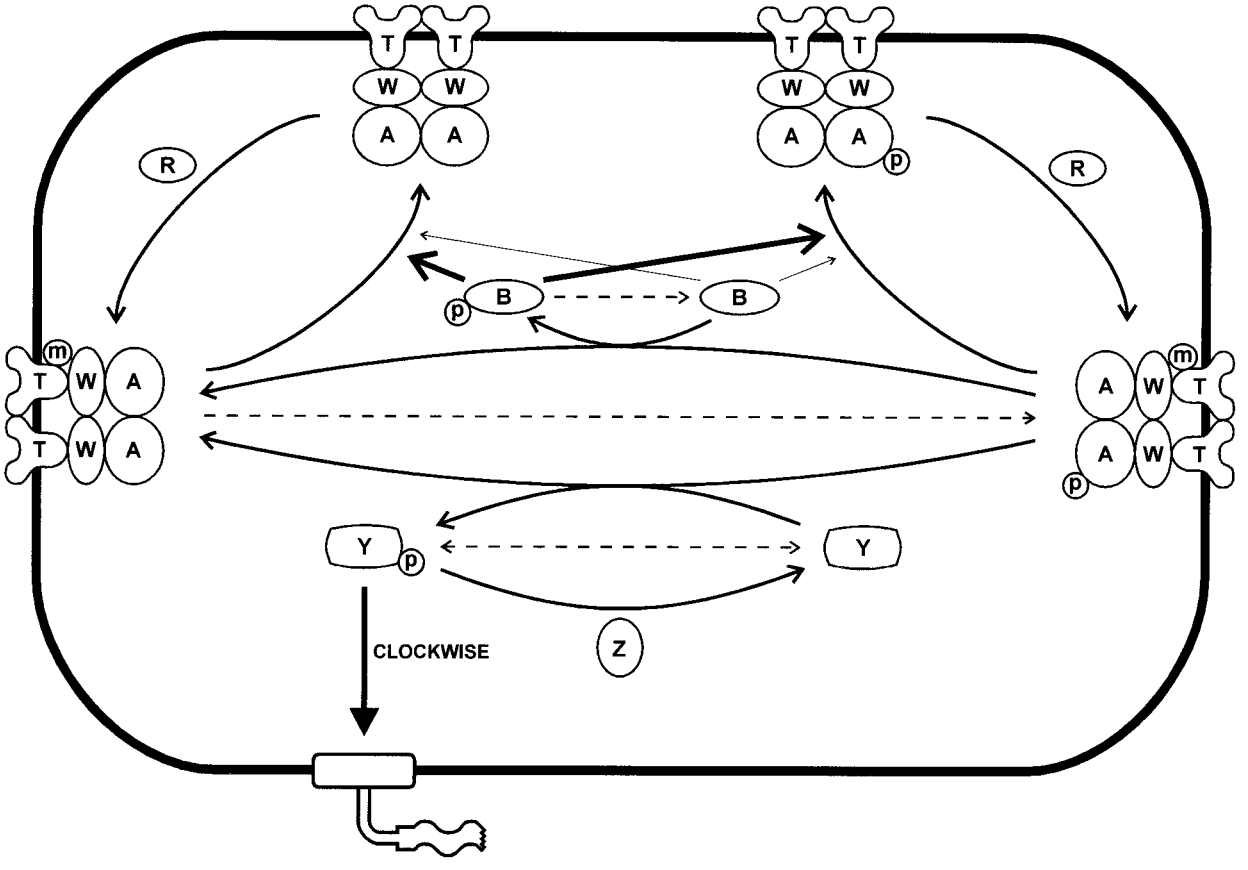

FIGURE 1 Signal transduction pathway in bacterial chemotaxis. The seven chemotaxis proteins, Tar, CheR, CheB, CheW, CheA, CheY, and CheZ, are represented by the symbols, T, R, B, W, A, Y, and Z, respectively, with methylation and phosphorylation represented by the symbols m and p, respectively. Solid arrows indicate enzyme-catalyzed reactions; dashed arrows indicate autocatalysis. Note that the scheme presented is for the robust version of the pathway, in which only methylated receptor complexes are permitted to undergo autophosphorylation and phosphotransfer. Unmethylated receptor complexes may participate in these reactions only in the fine-tuned version of the pathway.

The "output" of the computer simulations is the cytoplasmic concentration of the phosphorylated species CheYp, which interacts with a switching complex on the cytoplasmic face of the flagellar motor to reverse its direction of rotation. Present evidence suggests that this is a cooperative interaction in which many CheYp molecules bind to FliM molecules in the switch complex of the motor (Welch et al., 1993). In this study, we assume that the relationship between the CheYp concentration and motor bias is of the form:

$$\text{bias} = 1 - \frac{[\text{CheYp}]^{5.5}}{17/3[\text{CheYp}]_{\text{wt}}^{5.5} + [\text{CheYp}]^{5.5}} \qquad (1)$$

An early study, in which CheY was expressed at different levels in a bacterial strain otherwise devoid of Che proteins, led to an estimated Hill coefficient for the interaction 5.5 ± 1.9 (Kuo and Koshland, 1989); "wt" signifies the CheYp concentration that would produce a bias of 0.85 in a wild-type cell.

Tethering experiments

E. coli cells wild-type for chemotaxis (RP437) were tethered to glass coverslips by their shorn flagella (Bray et al., 1993). The movements of individual cells, along with a computer-readable timecode, were recorded onto videotape for a minimum of 30 s, using a rate of 60 frames per second. The tape was played back at 12 frames per second, while changes in the direction of rotation were manually logged using specialized computer software (Observer, Noldus Information Technology, The Netherlands). Rotational bias was calculated as the fraction of time the cell was rotating counterclockwise. A comparison of bias distributions from different cultures demonstrated there was no significant variation between cultures.

RESULTS

Changing individual proteins

An important feature of the computer model used in this study is that it includes the network of binding steps leading to the formation of the receptor complex (Bray and Bourret, 1995). Other models of chemotaxis (Hauri and Ross, 1995; Barkai and Leibler, 1997) lack this feature, and treat the receptor complex as a fixed unit in their simulations. We have used the greater flexibility our model provides to examine the effects of mutations in receptor function, and adaptation mechanism, on the individuality question. This gives us the opportunity to examine the effects of changing the levels of all seven individual components of the pathway on the steady-state levels of CheYp, including Tar, CheA, and CheW.

As a first step, we considered the effect of changing the concentration of each protein in turn while keeping the concentrations of the other six proteins constant. The results for the fine-tuned adaptational pathway over a range of expression from zero to 10× wild-type are presented in Fig. 2 *A*. Three proteins (Tar, CheW, and CheA) display a maximum CheYp concentration when expressed at, or close to, the wild-type level; two proteins (CheZ and Che B) display a negative gradient (that is, a decrease in CheYp concentration with increasing protein level); and the two remaining proteins (CheR and CheY) display a positive gradient.

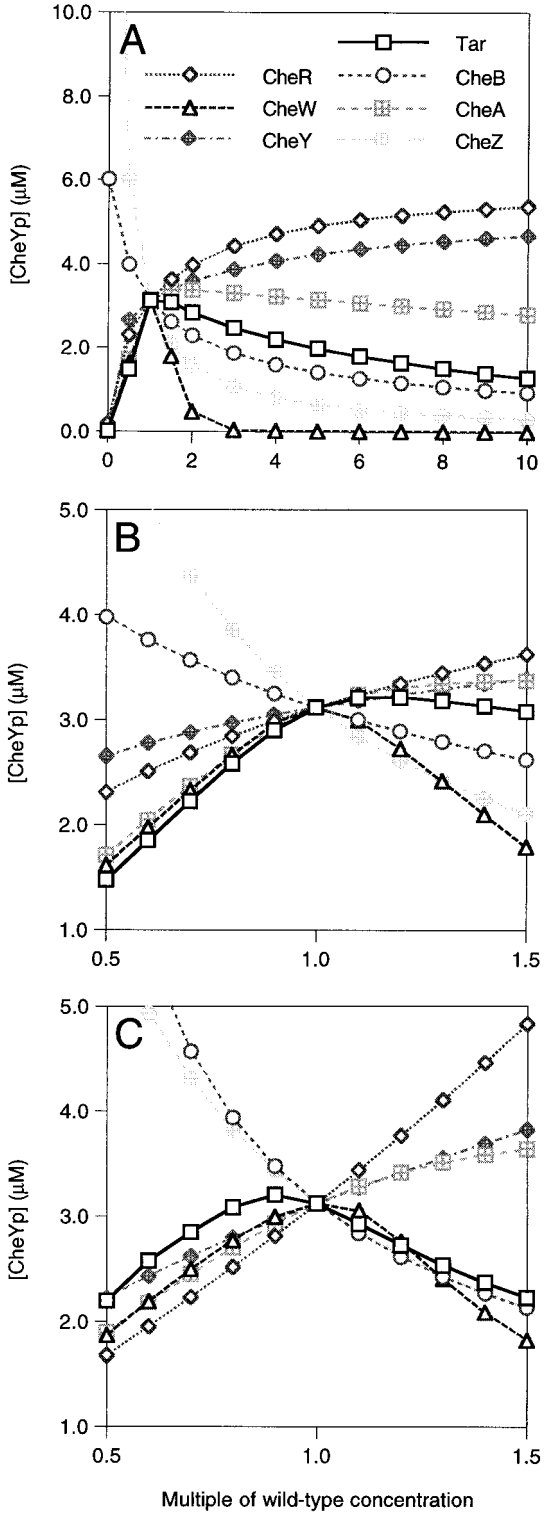

FIGURE 2 Predicted effect of changes in the expression of single genes on intracellular CheYp concentration. The level of each protein in turn is varied by fixed amounts while the remaining six proteins are held at their wild-type levels. (*A*) Simulation of the effects of changing each protein from 0 to 10 times wild-type levels using the fine-tuned adaptation algorithm. Note that each protein has a distinct effect as its intracellular concentration is increased. (*B* and *C*) Predicted CheYp concentrations produced by levels of chemotaxis proteins between 0.5 and 1.5 times wild-type with the fine-tuned [as in (*A*)] and the robust adaptation algorithms, respectively.

The existence of a maximum CheYp in the case of Tar, CheW, and CheA is consonant with the experimental observation that both null and overexpression mutants affecting these proteins display a high bias (Liu and Parkinson, 1989; Sanders et al., 1989). The mechanistic basis for this maximum has been proposed to lie in the network of binding reactions leading to formation of the Tar complex (Bray and Bourret, 1995). The negative gradient obtained with CheZ and CheB may also be understood on the basis of the signal transduction pathway shown in Fig. 1. Since CheZ is the specific phosphatase of CheY, high levels of CheZ will reduce the levels of CheYp and thereby increase the bias. CheB catalyzes the removal of methyl groups from the Tar complex, and this lowers the rate of phosphorylation of CheY. Increasing CheB, therefore, leads to a decrease in CheYp.

In the case of the two positive gradients, that of CheR has a similar explanation to CheB—high levels increase methylation of the Tar complex and hence increase CheYp. Increases in CheY expression, however, operate by a more subtle mechanism. Since CheA autophosphorylation is rate-limiting with respect to phosphotransfer, and almost all of the phosphate flux is directed toward CheY rather than CheB, a large increase in CheY will increase CheYp only marginally, but reduce CheBp by a substantial amount. As CheBp is many times more active than CheB, this reduction in total methylesterase activity with unchanged methyltransferase activity will increase the degree of methylation of the Tar complex, which will feed through into the observed increase in CheYp.

The fine-tuned and robust adaptational mechanisms produced similar but not identical results in the deterministic simulations (Fig. 2, *B* and *C*, respectively). The more limited range of protein expression in comparison with Fig. 2 *A* reveals differences in the respective positions of the maxima for Tar, CheW, and CheA.

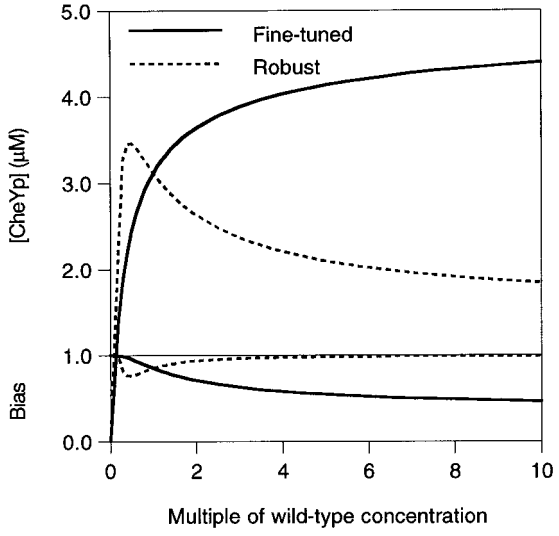

FIGURE 3 Predicted effect of changes in the coordinate expression of all seven genes on the CheYp concentration and the associated bias. Note the dramatic difference in the results produced at high concentration between the robust and fine-tuned algorithms.

Changing proteins in concert

It is evident from the data in Fig. 2 that individual chemotaxis proteins may have opposite effects on the CheYp levels. The question therefore arises whether increases or decreases in multiple proteins simultaneously would result in these effects canceling out. We therefore examined the consequences of increasing or decreasing all seven signaling proteins in concert. Changes of this kind could occur naturally as the *mocha* and *meche* operons, which carry the structural genes for all of the proteins under investigation, are expressed at different levels through changes in the nutritional status of the bacterium (Silverman and Simon, 1974).

The effect of coordinate changes was found, in fact, to lie within the extremes of the range shown by individual proteins (Fig. 3). There was, however, an unexpected sensitivity to the method of adaptation incorporated in the program. As the coordinate concentration is increased from zero, both pathways initially display increasing CheYp concentrations, but it is only with the robust algorithm that the CheYp concentration passes through a maximum before declining. At high coordinate concentrations, this results in the fine-tuned algorithm producing a response at the opposite end of the bias spectrum to that produced by the robust algorithm.

With the exception of some earlier studies of the effects of CheY overexpression on swimming behavior (Kuo and Koshland, 1989), there has been no systematic investigation of the effects of different levels of expression of the chemotaxis signaling proteins on resting bias. Our results suggest that such a study would be highly informative, and in particular might help to distinguish between the possible models of the adaptation process.

Changing proteins randomly

The most likely origin of individuality in coliform swimming behavior lies in independent variation in each chemotaxis protein from cell to cell. Although there is little direct evidence for this conjecture, it is well known that the protein content of individual cells, even from a cloned population, shows substantial variation. Experiments using flow cytometry typically reveal that the protein content per cell has a standard deviation in excess of 10% of the mean (see, for example, Darzynkiewicz et al., 1982; Crissman et al., 1985). Changes of this kind could arise as a consequence of unequal partitioning of protein molecules at cell division (Sennerstam, 1988); or they could be due to stochastic mechanisms in gene expression (Ko, 1992), with occasional large bursts of signal proteins activating or suppressing controlled genes, thereby triggering cascades or affecting the decision between switching alternatives (McAdams and Arkin, 1997). To simulate this effect we selected the concentrations

of all the chemotaxis proteins at random from independent normal distributions with equal relative standard deviations.

The range of CheYp concentration was computed for a population of bacteria in which each of the seven chemotaxis proteins was subject to independent variation in concentration (Fig. 4 *A*). In Fig. 4 *B*, we have used these CheYp values to calculate the expected rotational bias of the flagellar motors of the cells according to Eq. 1. It may be seen that the spread of CheYp values and bias values increases markedly with increasing relative standard deviation of protein copy number.

Thus, if we arbitrarily define a bias falling between 0.8 and 0.9 as wild-type, then with 5% standard deviation of protein copy number ~55% of cells will be wild-type, whereas with 10% standard deviation only 28% will be wild-type. The above distributions were calculated using the robust adaptational algorithm, but the fine-tuned algorithm gave very similar results (not shown).

The strength of any computer model lies in its ability to reproduce experimental results. As a consequence, we determined experimentally the bias distribution of a large sample of wild-type cells drawn from a genetically identical population (see Methods), and compared this data with the computer-generated result. In Fig. 5 *A*, we present the distribution of bias values obtained from 500 individual cells compared to the distribution predicted from the computer program with a standard deviation of 10% of the mean (from Fig. 4 *B*). In Fig. 5 *B*, the experimental data have been used to deduce the probable concentration of CheYp in each

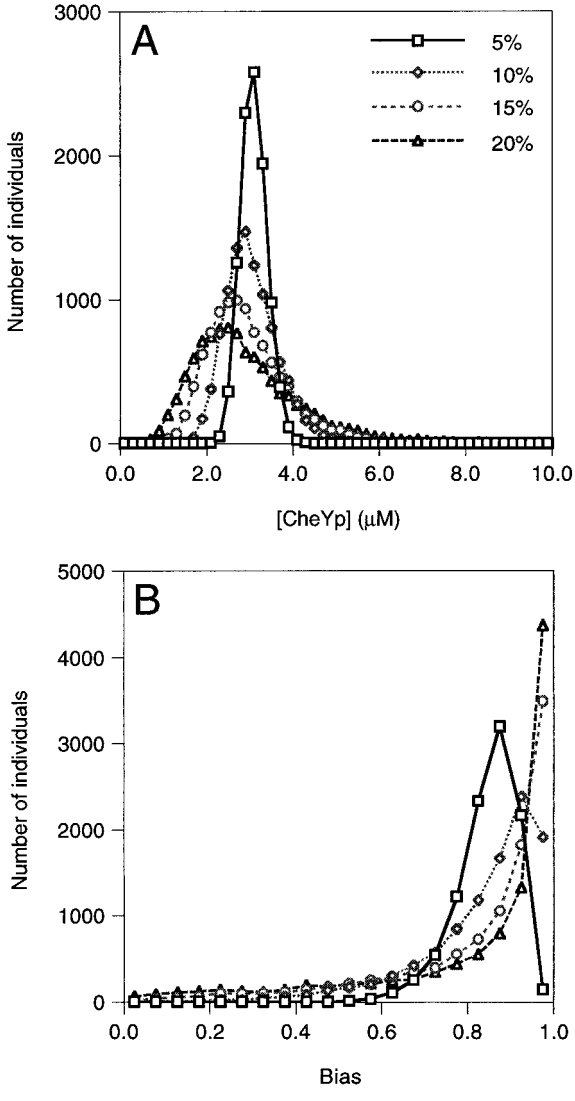

FIGURE 4 Predicted distribution of CheYp concentrations and biases of populations of the wild-type strain. Receptor modification reactions were implemented by the robust algorithm. (*A*) Distributions of CheYp concentrations are shown for a range of relative standard deviations of protein concentration. (*B*) Distributions of rotational bias were calculated from the CheYp concentrations shown in (*A*) using the relationship given in Eq. 1. The population in each simulation consisted of 10,000 individuals.

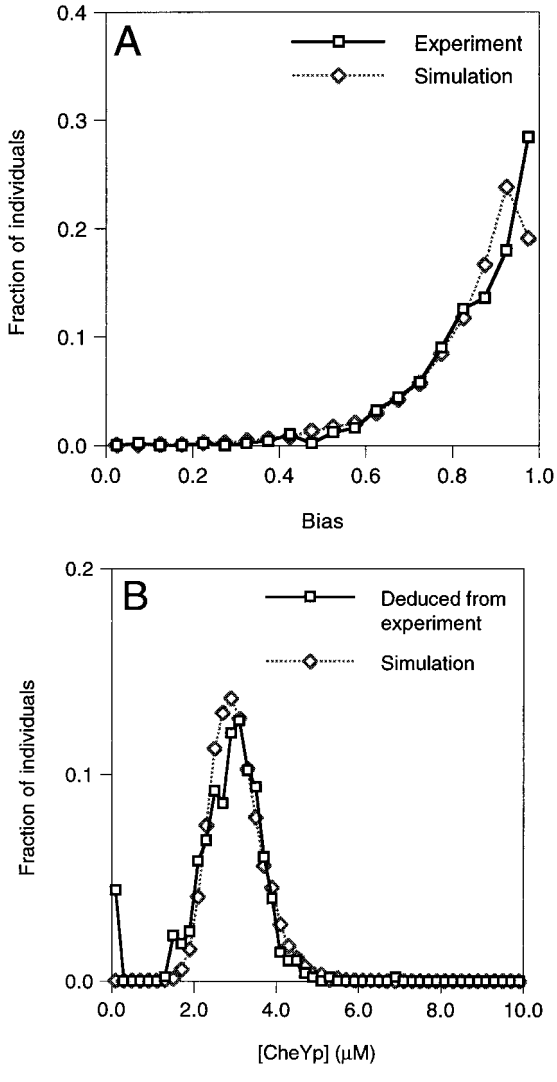

FIGURE 5 Comparison of theory and experiment. (*A*) The distribution of rotational biases measured in 500 tethered bacteria is compared to the simulated distribution of biases of 10,000 wild-type bacteria. The simulated distribution was obtained using a 10% standard deviation in protein copy number. (*B*) Comparison of intracellular CheYp concentrations deduced from the experimentally observed rotations (using Eq. 1) to those predicted by the computer simulation using the robust algorithm.

cell from Eq. 1, and this is shown together with the computed distribution with the same standard deviation of 10% (from Fig. 4 *A*).

In both Fig. 5 *A* and 5 *B*, it may be seen that the experimental and computed distributions are broadly similar. The number of cells with a nominal wild-type swimming bias, for example, was 26% in the experimental population and 28% for the computed distribution. On the basis of this result, therefore, we are able to say that the observed variation in swimming behavior from cell to cell in this population of bacterial cells could have arisen if the numbers of seven chemotaxis proteins fluctuated randomly with a standard deviation of 10% of the mean.

Mutant distributions

We were curious to know whether mutant bacteria in which one or more of the proteins controlling swimming have been altered by mutation would show more or less individual variation than wild-type cells. The comparison is especially informative in mutant strains that, while being unable to respond correctly to attractants or repellents, nevertheless have an average unstimulated bias close to wild-type values. Two mutants of this kind were modeled in this study: the first is an R^-B^- strain that lacks both the methylating enzyme CheR and the demethylating enzyme CheB and is, therefore, defective in the adaptation response; the second is a $T^-W^-Z^-$ strain lacking the Tar receptor, CheW and CheZ.

Predicted CheYp distributions for populations of these two mutants compared to those of the wild-type strain are shown in Fig. 6 *A* (the robust adaptation algorithm) and Fig. 6 *B* (the fine-tuned algorithm). These results were calculated for a 10% standard deviation in protein numbers per cell. In general, as shown in Fig. 6 and Table 1, the difference between the mutant and the wild-type cells is not very great. The $T^-W^-Z^-$ strain displays a slightly narrower distribution of CheYp concentrations than the R^-B^- strain with both the fine-tuned and robust algorithms. The R^-B^- strain only displays a narrower distribution of CheYp concentrations than the wild-type strain with the robust algorithm—there is little difference between the two distributions produced with the fine-tuned algorithm.

For the mutant strains, both the robust and fine-tuned adaptation algorithms produce almost identical distributions of CheYp concentrations because of the absence of receptor modification activity: the $T^-W^-Z^-$ strain lacks receptor complexes, while the R^-B^- strain lacks the modification enzymes themselves. The difference between the two mutant strains lies in the mechanism for generating the phosphate flux: in the $T^-W^-Z^-$ strain, by the slow autophosphorylation of free CheA dimers; in the R^-B^- strain, by the rapid autophosphorylation of methylated Tar complexes. The magnitude of the flux in the $T^-W^-Z^-$ strain is linearly dependent on the CheA concentration, but in the R^-B^- strain it is a nonlinear function of the Tar, CheW, and CheA

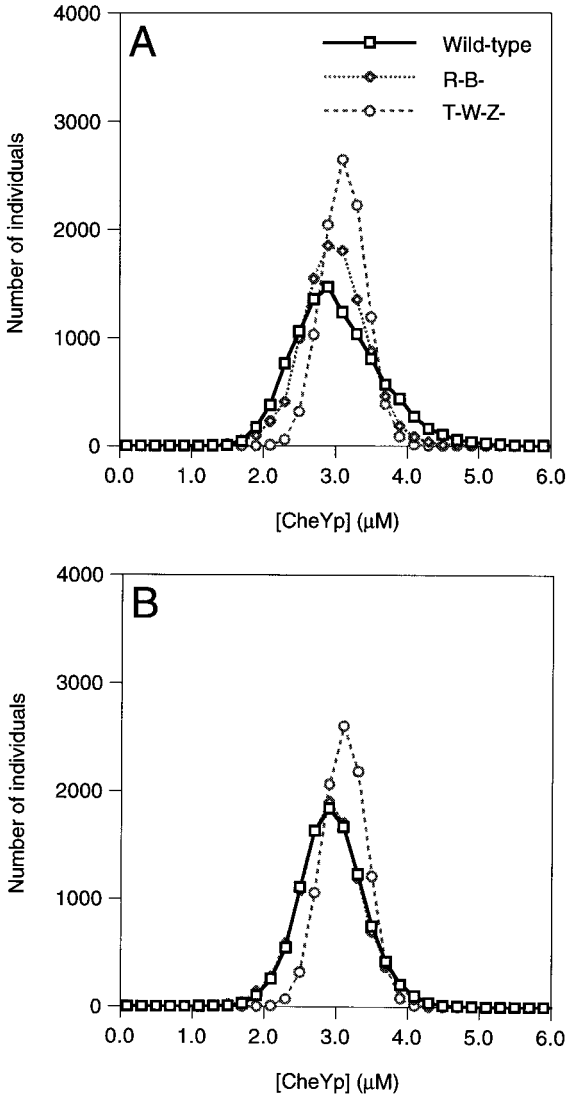

FIGURE 6 Predicted bias distribution of populations of three strains with the receptor modification reactions implemented by (*A*) robust and (*B*) fine-tuned algorithms. The population in each case consisted of 10,000 individuals, all with a standard deviation of protein copy number of 10%.

concentrations determined by the K_d values of the network of binding steps. The synergistic effect of random changes in the concentration of all three components of the complex widens the CheYp distribution with respect to the $T^-W^-Z^-$ strain (Fig. 2 illustrates the deterministic effect with each of these components taken in turn).

TABLE 1 Bias distributions of wild-type and mutant populations

Population	Robust Algorithm	Fine-Tuned Algorithm
Wild-type	0.84 ± 0.14* (28%)[#]	0.86 ± 0.10 (37%)
R^-B^-	0.86 ± 0.09 (40%)	0.87 ± 0.09 (44%)
$T^-W^-Z^-$	0.84 ± 0.07 (56%)	0.84 ± 0.07 (56%)

*Mean and standard deviation of the population.
[#]Fraction of the population with a bias in the range of 0.8 to 0.9.

Experimental predictions

An important feature of the detailed, molecular-based computer simulations used in this study is that they readily provide specific predictions that can be tested experimentally. For example, the bias distribution seen in populations of both the R^-B^- strain and the $T^-W^-Z^-$ strain should have a comparable standard deviation to that of a population of wild-type cells. Until recently, it has not been feasible to perform such experiments due to the inordinate amount of time involved in quantifying the biases of large numbers of tethered cells. The use of automated tracking equipment on this task would enable large sets of bias data to be obtained in much shorter periods of time.

This work was supported by a grant from the UK Medical Research Council to Dennis Bray.

REFERENCES

Asakura, S., and H. Honda. 1984. Two-state model for bacterial chemoreceptor proteins: the role of multiple methylation. *J. Mol. Biol.* 176: 349–367.

Barkai, N., and S. Leibler. 1997. Robustness in simple biochemical networks. *Nature.* 387:913–917.

Berg, H. C., and D. A. Brown. 1972. Chemotaxis in Escherichia coli analysed by three-dimensional tracking. *Nature.* 239:500–504.

Block, S. M., J. E. Segall, and H. C. Berg. 1983. Adaptation kinetics in bacterial chemotaxis. *J. Bacteriol.* 154:312–323.

Bray, D., and R. B. Bourret. 1995. Computer analysis of the binding reactions leading to a transmembrane receptor-linked multiprotein complex involved in bacterial chemotaxis. *Mol. Biol. Cell.* 6:1367–1380.

Bray, D., R. B. Bourret, and M. I. Simon. 1993. Computer simulation of the phosphorylation cascade controlling bacterial chemotaxis. *Mol. Biol. Cell.* 4:469–482.

Crissman, H. A., Z. Darzynkiewicz, R. A. Tobey, and J. A. Steinkamp. 1985. Correlated measurements of DNA, RNA, and protein in individual cells by flow cytometry. *Science.* 228:1321–1324.

Darzynkiewicz, Z., H. Crissman, F. Traganos, and J. Steinkamp. 1982. Cell heterogeneity during the cell cycle. *J. Cell. Physiol.* 113:465–474.

Eisenbach, M. 1990. Functions of the flagellar modes of rotation in bacterial motility and chemotaxis. *Mol. Microbiol.* 4:161–167.

Eisenbach, M. 1996. Control of bacterial chemotaxis. *Mol. Microbiol.* 20:903–910.

Hauri, D. C., and J. Ross. 1995. A model of excitation and adaptation in bacterial chemotaxis. *Biophys. J.* 68:708–722.

Ko, M. S. H. 1992. Induction mechanism of a single gene molecule: stochastic or deterministic. *BioEssays.* 14:341–346.

Kuo, S. C., and D. E. Koshland, Jr. 1989. Multiple kinetic states for the flagellar motor switch. *J. Bacteriol.* 171:6279–6287.

Liu, J., and J. S. Parkinson. 1989. Role of CheW protein in coupling membrane receptors to the intracellular signalling system of bacterial chemotaxis. *Proc. Natl. Acad. Sci. USA.* 86:8703–8707.

McAdams, H. H., and A. Arkin. 1997. Stochastic mechanisms in gene expression. *Proc. Natl. Acad. Sci. USA.* 94:814–819.

Parkinson, J. S. 1993. Signal transduction schemes of bacteria. *Cell.* 73:857–871.

Sanders, D. A., B. Mendez, and D. E. Koshland, Jr. 1989. Role of the CheW protein in bacterial chemotaxis: overexpression is equivalent to absence. *J. Bacteriol.* 171:6271–6278.

Segel, L. A., A. Goldbeter, P. N. Devreotes, and B. E. Knox. 1986. A mechanism for exact sensory adaptation based on receptor modification. *J. Theor. Biol.* 120:151–179.

Sennerstam, R. 1988. Partition of protein (mass) to sister cell pairs at mitosis: a re-evaluation. *J. Cell Sci.* 90:301–306.

Silverman, M., and M. I. Simon. 1974. Characterization of Escherichia coli flagellar mutants that are insensitive to catabolite repression. *J. Bacteriol.* 120:1196–1203.

Spiro, P. A., J. S. Parkinson, and H. G. Othmer. 1997. A model of excitation and adaptation in bacterial chemotaxis. *Proc. Natl. Acad. Sci. USA.* 94:7263–7268.

Spudich, J. L., and D. E. Koshland, Jr. 1976. Non-genetic individuality: chance in the single cell. *Nature.* 262:467–471.

Stock, J. B., and M. G. Surette. 1996. Chemotaxis. *In* Escherichia coli and Salmonella: Cellular and Molecular Biology. F. C. Neidhardt, editor. American Society for Microbiology, Washington, D.C. 1103–1129.

Welch, M., K. Oosawa, S.-I. Aizawa, and M. Eisenbach. 1993. Phosphorylation-dependent binding of a signal molecule to the flagellar switch of bacteria. *Proc. Natl. Acad. Sci. USA.* 90:8787–8791.